Deep-Sea Research II 93 (2013) 159–168

Contents lists available at SciVerse ScienceDirect

Deep-Sea Research II

journal homepage: www.elsevier.com/locate/dsr2

The response of phytoplankton to climate variability associated with the North Atlantic Oscillation

Li Zhai [a],*, Trevor Platt [b], Charles Tang [a], Shubha Sathyendranath [b], Antony Walne [c]

[a] *Bedford Institute of Oceanography, Canada*
[b] *Plymouth Marine Laboratory, UK*
[c] *Sir Alister Hardy Foundation for Ocean Science, UK*

ARTICLE INFO

Available online 9 April 2013

Keywords:
Phytoplankton
Spring blooms
North Atlantic Oscillation
Inter-annual variation
CPR
Ocean colour

ABSTRACT

Inter-annual variability in the timing of phytoplankton spring bloom and phytoplankton community structure in the central North Atlantic Ocean was quantified using ocean color data and continuous plankton recorder (CPR) data. This variability was related to the North Atlantic Oscillation using correlation analysis and multivariate auto-regression models. The initiation of the spring bloom derived from CPR phytoplankton color index data is similar to that derived from satellite chlorophyll, and exhibits a nominal correlation with the sea surface temperature (SST) and the North Atlantic Oscillation (NAO). The extrapolated spring bloom timing suggested later initiation of blooms in the mid-1980s and earlier initiation of blooms in the 1990s. The climatological phytoplankton community structure in the central North Atlantic is dominated by diatoms, except for a shift in community composition favoring dinoflagellates in August. The ratio of diatoms to total phytoplankton abundance and the ratio of dinoflagellates to total phytoplankton abundance are both closely correlated with the NAO and SST. The extended time series of phytoplankton community structure between 1985 and 2009, deduced from the time series of SST and NAO over the same interval, showed a decadal shift away from diatoms towards dinoflagellates. The linkages between the NAO, and changes in stratification and phytoplankton processes occur over a larger scale than previously observed.

1. Introduction

To assist ecosystem-based management decisions, we need to develop objective metrics, called ecological indicators (Platt and Sathyendranath, 2008). One such ecological indicator is phytoplankton phenology, defined as the timing and magnitude of the seasonal phytoplankton cycle, in which the dominant event is the spring bloom in temperate latitudes. Inter-annual fluctuations in the phase of the cycle are important for the marine ecosystem. Ocean-color radiometry is ideal for deriving phytoplankton phenology in the pelagic system of the ocean. Phytoplankton phenology, as determined by ocean-color radiometry, has a wide variety of applications, including fisheries management (Platt et al., 2003; Koeller et al., 2009), the study of carbon cycles mediated by phytoplankton (Zhai et al., 2010), and understanding the effect of phytoplankton on the heat budget of the upper ocean (Zhai et al., 2011a). However the time series record that can be recovered from remote sensing is still reasonably short (about 15 years). Because the phenological pattern has a physical basis (i.e., onset of stratification), we need to reconstruct through retrospective physical analyses, the onset of stratification and its relation to phytoplankton phenology, with a view to extending the phenologic record and therefore assess relationships with low frequency climate modes.

There are two suitable sources of data for characterizing inter-annual variability in phytoplankton seasonality. They are the continuous plankton recorder (CPR) and satellite ocean-color data, both of which provide complementary ways of monitoring phytoplankton in the ocean (Head and Pepin, 2010b). The CPR sampling is the most extensive marine monitoring program and provides a long time series, starting in 1931 (Richardson et al., 2006), of semi-quantitative estimates of total chlorophyll and abundance of phytoplankton species. Advantages of ocean color data include its planar view and high spatial and temporal resolution, though time series are much shorter. Ocean color data are based on strict radiometric measurements, which are interpreted as concentrations of chlorophyll-*a*, a quantitative and objective metric for a fundamental property of the marine ecosystem, namely the autotrophic biomass.

CPR data have been used to demonstrate that fluctuations in phytoplankton abundance and community structure are tightly linked to physical forcing. Significant linear trends in phytoplankton color index (PCI), observed in the northeast Atlantic and North Sea from 1948 to 1995, potentially reflect a response to climate forcing (Reid et al., 1998). Seasonal cycles of dinoflagellates in North Sea occur earlier in the year from 1958 to 2002, and showed highly

---

* Corresponding author.
E-mail address: Li.Zhai@phys.ocean.dal.ca (L. Zhai).

0967-0645/$ - see front matter © 2013 Elsevier Ltd. All rights reserved.
http://dx.doi.org/10.1016/j.dsr2.2013.04.009

significant correlations with the sea surface temperature (SST) during this period (Edwards and Richardson, 2004). In transition zones between gyre systems of the northeast Atlantic, the variability in phytoplankton community structure can be driven by opposing North Atlantic Oscillation (NAO) phases (Henson et al., 2012). The majority of studies using CPR data have focused on the most consistently sampled regions of the northeast Atlantic and the North Sea, but only a few studies have focused on the northwest Atlantic Ocean. For example, on the Scotian shelf, physical factors including storms, temperature, and stratification explained 20–40% of the observed variance in phytoplankton taxa (Sameoto, 2001). The increases in the abundance of phytoplankton in the 1990s on the Newfoundland and Scotian shelf are believed to be a response to the persistent freshening of the water column, and consequent increased stratification (Head and Sameoto, 2007). In the subpolar gyre, phytoplankton increased with rising temperatures during 1990s and 2000s, which was also explained by increased stratification (Head and Pepin, 2010a).

Ocean color data have been used to examine phytoplankton pheno-logy at both regional and global scales. Seasonally-increasing vertically-averaged light in the mixed layer, an essential property in Sverdrup's theory (Sverdrup, 1953), triggers spring blooms on the Northwest Atlantic Shelf and around Iceland (Platt et al., 2009; Zhai et al., 2011b, 2012). In addition, large inter-annual variability in the duration of the growing period of phytoplankton was observed in the global ocean and associated with SST anomalies (Racault et al., 2012). For example, in the subarctic North Atlantic the variability of coccolithophore abundance was shown to be related to physical variables SST, mixed-layer depth and light intensity (Raitsos et al., 2006). In contrast, in the Irminger Basin, the timing and magnitude of the spring bloom depend on winter pre-conditioning (Henson et al., 2006).

These previous studies have greatly improved our understanding of marine ecosystem dynamics in the North Atlantic Ocean. Their authors have suggested that future studies should focus on a specific region in order to gain a better understanding of changes in physical forcing and phytoplankton response. In this study, we focus on the North Central Atlantic Ocean from 45°N to 65°N and 20°W to 50°W (Fig. 1). The reasons for choosing this region are threefold: (1) the region is continuously sampled by the CPR program after 1991; (2) the majority of CPR shipping routes lies close to the transition zone between two ecological provinces; and (3) the NAO forcing is expected to have a significant effect on the physical environment in this region, which we hypothesize impacts on phytoplankton phenology.

The CPR transects used in this analysis pass through three ecological provinces, as defined in Longhurst (2007), including the Boreal Polar Province (BPLR), the Atlantic Arctic Province (ARCT) and the North Atlantic Drift Province (NADR). A line from Iceland to the Flemish Cap, closely coinciding with major CPR shipping routes, divides the Arctic Province to the north from North Atlantic Drift Province to the south. BPLR is bounded by a front at the edge of the Greenland coastal current and has varying periods of sea-ice coverage. The surface circulation in ARCT is dominated by a cyclonic subpolar gyre. The North Atlantic Current sends one branch north into ARCT as the Irminger Current; some of this flow turns westwards along the east Greenland Sea and eventually flows into the eastern Labrador Sea. An acknowledged limitation of Longhurst's classification of ecological provinces lies in the static definition of the province boundaries, given that water mass boundaries change in response to physical forcing (Platt and Sathyendranath, 1999; Devred et al., 2007). In this study, we show that dynamic province boundaries derived from satellite observations are useful as an aid to interpretation of the CPR data.

The objective of this study was to quantify inter-annual variations of phytoplankton abundance and assemblage composition in the central North Atlantic using both CPR and satellite data sets and to explain these fluctuations in their physical context. We examine the statistical relationships between variability in sea surface temperature and phytoplankton community structure and the initiation of the spring bloom in the central North Atlantic, and show that they can be interpreted through climate forcing of the NAO. The underlying physical mechanism of vertical stratification, caused by wind-induced vertical mixing and large-scale horizontal advection, is suggested to explain the observed relationships between the NAO, SST and phytoplankton variability. A multivariate regressive model is developed as a method to extend retrospectively the estimation of spring bloom initiation and community structure.

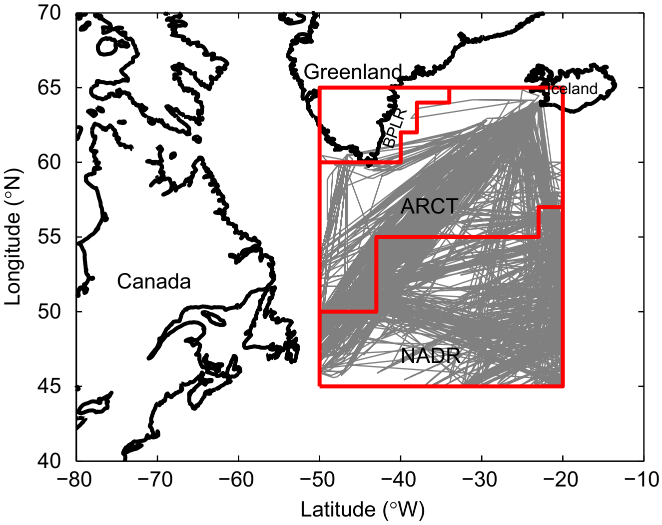

Fig. 1. The study area, the central North Atlantic, consists of three ecological provinces defined in Longhurst (2007), including Boreal Polar Province (BPLR), Atlantic Arctic Province (ARCT) and North Atlantic Drift Province (NADR). The CPR ship routes are marked in gray lines.

2. Data and methods

2.1. CPR data

The CPR survey exploits the opportunity provided by merchant ships on their normal trading routes to collect plankton continuously from a mean towed depth of 6.7 m (Batten et al., 2003b). A detailed description of the CPR design and sample processing has been documented by Richardson et al. (2006). The CPR has a nominal mesh size of 270 μm and in principle under-samples smaller phytoplankton species, however, some smaller phytoplankton are regularly captured in CPR samples. This is possibly due to the leno weave of the relatively thick silk strands in the mesh, or an effect of clogging by phytoplankton and zooplankton, both of which reduce the effective mesh size. CPR data should not be used as an absolute measure of abundance, but as semi-quantitative estimates that reflect real inter-annual and seasonal patterns of phytoplankton dynamics (Richardson et al., 2006).

In this study, CPR data collected between 1991 and 2009 were used because this time period has the best coverage of shipping routes in the Central North Atlantic (http://www.sahfos.ac.uk/), here defined as 45°N–65°N and 20°W–50°W. CPR data were processed for this analysis as follows. First, CPR data for each month in each year were averaged over the study area, and then the monthly time series in each calendar year was used to calculate the annual mean for each year. It was recommended that at least eight months need to be sampled in a year to have an adequate estimate of the seasonal cycle to estimate the annual abundance (Richardson et al., 2006), and each year of this analysis has at least eight months (see Figs. 4A and 6). By calculating this way, the yearly mean is weighted by the number of samples used to calculate each monthly mean of CPR data (Barton et al., 2003). Similar to previous studies (Barton et al., 2003; Head and Pepin, 2010b), simple linear interpolation is used to fill in the values of PCI, diatom and dinoflagellate ratios for missing months.

The PCI is recommended as a semi-quantitative estimate of total phytoplankton biomass as a strong positive relationship between PCI and fluorometrically-determined chlorophyll-*a* (Batten et al., 2003a) as well as satellite chlorophyll-*a* (Raitsos et al., 2005) has been demonstrated. A numerical value was assigned to each sample to indicate the phytoplankton abundance, according to the intensity of the green color index (Colebrook and Robinson 1961, 1965): 0 for no color; 1.0 for very pale green; 2.0 for pale green; and 6.5 for green, were assigned. Despite the semi-quantitative nature of the PCI, it is considered the best estimate of total phytoplankton biomass from CPR data (Richardson et al., 2006). The onset of the spring bloom was defined as the time when the PCI first increased to the mean of the yearly time series of PCI within a year.

The first comprehensive list of all phytoplankton taxa in the CPR database is provided by Richardson et al. (2006, Table 5). In the North Central Atlantic, the CPR survey identified and recorded a total of 143 phytoplankton taxa, including 56 total dinoflagellate species and 63 total diatom species. We defined two simple phytoplankton community indices: one is the ratio of diatom abundance to total phytoplankton taxa; another is the ratio of dinoflagellate abundance to total phytoplankton taxa. The derived diatom and dinoflagellate ratios reflect their relative abundance in terms of cell numbers, but do not take into account relative carbon contribution by each group.

2.2. Satellite data

The satellite chlorophyll-*a* data extracted for the study area are from global archives of the 9-km SeaWiFS level-3 binned 8-day chlorophyll concentration for the period from 1997 to 2009 (http://oceancolor.gsfc.nasa.gov/), estimated using the Ocean Chlorophyll 4—version 4 (OC4) algorithm (O'Reilly et al., 1998). The SeaWiFS chlorophyll data are spatially averaged to get the 8-day time series representative of the study area. There are missing values in the SeaWiFS time series after the end of 2007, and linear interpolation was used to fill in the missing values. The onset of phytoplankton blooms was determined from the 8-day time series as the day of year when the chlorophyll concentration first rises to the mean of its annual time series.

Satellite-derived SST was extracted from the 4-km AVHRR (advanced very high resolution radiometer) Pathfinder 8-day sea surface temperature (SST) data for the period from 1985 to 2009. The satellite 8-day SST data were time-binned to provide images of mean annual SST, which were used to derive the dynamic boundaries of the provinces. The conventional, static boundaries of three ecological provinces in the study area (Fig. 1) were readjusted dynamically based on knowledge of the regional oceanography and that the instantaneous provincial boundaries will be found in the neighborhood of the static boundaries (Platt et al., 2005). To help interpret the CPR data, the boundary between the NADR and ARCT was readjusted to align with major CPR shipping routes. Here we define the BPLR as bounded by the 2 °C contour of the annual mean SST, and ARCT and NADR as separated by the 9 °C contour.

2.3. NAO index

The annual mean NAO index value was derived from the monthly NAO index during the period from 1985 to 2009, through a rotated principal component analysis of Northern Hemisphere monthly 500-mb height, following the procedure in Barnston and Livezey (1987) (http://www.cpc.ncep.noaa.gov/data/teledoc/teleindcalc.shtml).

2.4. Correlation analysis and multivariate auto-regression model

The relationship between phytoplankton and physical forcing was examined using Spearman R correlation analyses performed on mean annual values of the PCI, relative phytoplankton functional group abundance, SST and NAO index. Because our objective was to find the general relationship between climate forcing and phytoplankton phenology, a *p*-value less than 0.05 was accepted for a significant result, and a *p*-value less than 0.2 was accepted for a nominally significant result (Barton et al., 2003).

A multivariate auto-regression model was used to estimate and reconstruct the initiation of the spring bloom from the SST and NAO. The linear regression model is expressed as

$$Y_t = c + \sum_{i=0}^{n} (a_i T_{t-i} + b_i NAO_{t-i}) + \varepsilon_t, \tag{1}$$

where Y_t represents the initiation of the spring bloom in year *t*, *T* is the SST, *a*, *b* and *c* are constant coefficients, and ε is the residual. Eq. (1) was also applied to derive sets of regression coefficients for the diatom and dinoflagellate ratios. Here *n* is the order of the auto-regression model and is determined by the value at which the Akaike information criterion (AIC, Akaike, 1974) attains its minimum value. The AIC model-selection criterion (Fox, 2008) determines model structure by penalizing the fit for the number of parameters in the model and therefore will prefer a smaller model to a larger model. The AIC criterion (Fox, 2008) was employed due to its relative insensitivity to colinearity of model variables when present. Burnham and Anderson (2004) suggested an improvement on the AIC, called the bias-corrected AIC, which reduces small-sample bias and can be used in all cases:

$$AIC_c = (N-n)\log(\sigma^2) + 2q + \frac{2q(q+1)}{N-n-q-1'} \tag{2}$$

where *N* is the number of observations, σ^2 is the estimated residual variance, and *q* is the number of model variables plus the intercept. The correction term (the last term in Eq. 3) decreases as the ratio of sample size to number of parameters (*N/q*) increases. Smaller AIC values indicate a better-fitting model. We use κ^2 to denote the proportion of the observed variance accounted for by the statistical model with $0 \le \kappa^2 \le 1$, and defined as

$$\kappa^2 = \frac{\mathrm{var}(\tilde{Y}_t)}{\mathrm{var}(Y_t)}, \tag{3}$$

where $\tilde{Y}_t \equiv Y_t - \varepsilon_t$ is the estimated quantity from the auto-regression model.

3. Results

Using the AVHRR data from 1985 to 2009, we found a significant negative correlation between annual mean SST and the NAO index

Table 1
Matrix of correlation coefficients between the yearly North Atlantic Oscillation (NAO) index, sea surface temperature (SST), diatom ratio, dinoflagellate (Dino) ratio, initiation of spring bloom (Initiation), and phytoplankton color index (PCI).

	NAO	SST	Diatom ratio	Dino ratio	Initiation	PCI
NAO	1	**–0.62**[a]	**0.70**[a]	**–0.63**[a]	**–0.32**[b]	0.03
SST		1	**–0.65**[a]	**0.63**[a]	**0.33**[b]	0.03
Diatom ratio			1	**0.90**[a]	–0.11	0.03
Dino ratio				1	0.06	–0.06
Initiation					1	**–0.38**[b]
PCI						1

[a] $p < 0.005$.
[b] $p < 0.2$.

($r = -0.62$, $p < 0.001$, Table 1). To highlight the relationship between annual mean SST, the NAO and province boundaries, we compare 1998 a year with low NAO index and 1999 a year with high NAO index (Fig. 2). The white 9 °C contour defines the boundary between the Arctic and North Atlantic Drift provinces, which generally coincides with the CPR shipping routes from Newfoundland to Iceland, but in 1998 (Fig. 2B) the boundary was located further northeast of CPR tracks than in year 1999 (Fig. 2C). The longitudinal positions of the province boundary were averaged between 56 and 62°N, and the mean position is correlated with the NAO index

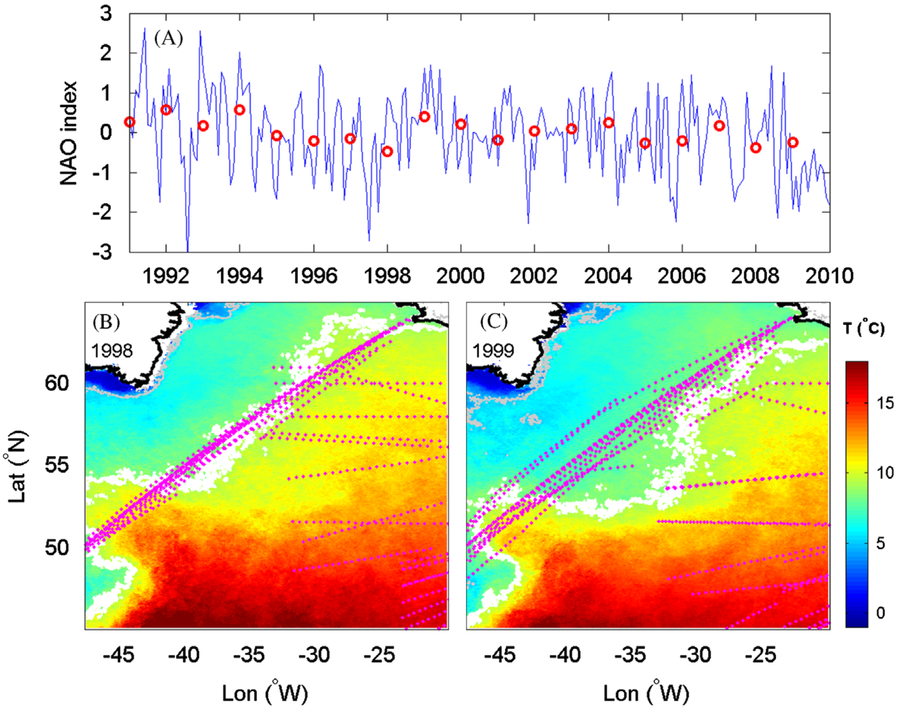

Fig. 2. (A) Monthly NAO index (blue line) and annual means (red circles) from year 1991 to 2009, (B) annual mean SST in 1998 and (C) annual mean SST in 1999. Dashed pink lines mark the cruise tracks. The white area is the 9 °C water, and gray area is the 5 °C water. (For interpretation of the references to color in this figure legend, the reader is referred to the web version of this article.)

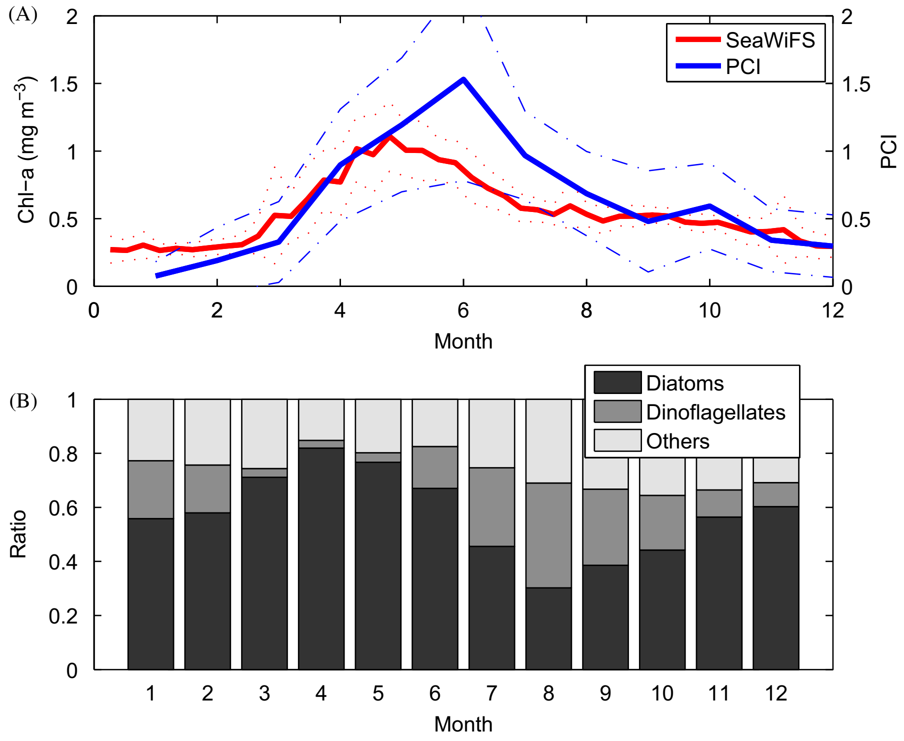

Fig. 3. (A) Seasonal variation of SeaWiFS chlorophyll-*a* (mg m^{-3}, blue line) and phytoplankton color index (PCI, red line). The standard deviations in each month are shown in dashed lines of the same color. (B) Relative contribution of diatoms, dinoflagellates, and other phytoplankton to the total phytoplankton abundance. The data are averaged for entire area shown in Fig. 1. (For interpretation of the references to color in this figure legend, the reader is referred to the web version of this article.)

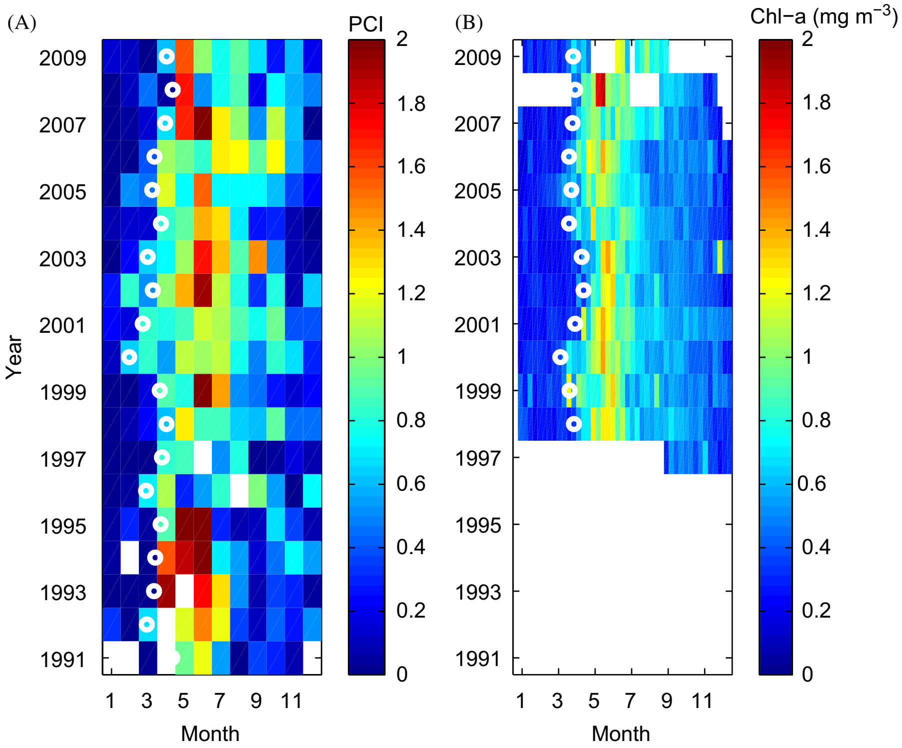

Fig. 4. (A) Mean monthly phytoplankton color index during 1991–2009 for the central North Atlantic. (B) Mean 8-day SeaWiFS Chlorophyll concentration during 1997–2009 for the central North Atlantic. White circles mark the initiation of spring bloom. (For interpretation of the references to color in this figure legend, the reader is referred to the web version of this article.)

(r=0.55, $p < 0.05$). This is not unexpected, as SST was used to define the province boundaries.

Satellites provide chlorophyll data at high temporal and spatial resolution, so it was of interest to consider the CPR data in relation to those from remote sensing. There was generally qualitative agreement between seasonal cycles (Fig. 3A) as measured by the CPR and as calculated from the satellite data, which is consistent with previous findings (Batten et al., 2003a,b; Raitsos et al., 2005; Head and Pepin, 2010b). The seasonal cycle of phytoplankton in the central North Atlantic is dominated by a single bloom in the spring. On average, the spring bloom (Fig. 3A) began in mid-March, reached peak amplitude in May, and lasted until August. The inter-annual variability of the seasonal signal was more pronounced in the CPR data than in the satellite data. The seasonal cycle of the diatom and dinoflagellate ratios (Fig. 3B) showed that diatoms are relatively more abundant in spring, whereas the relative abundance of dinoflagellates peaked in August.

The timing of the start of the spring bloom varied from year to year. Bloom initiation (Fig. 4) ranged from mid-March to late April, with earlier blooms in NAO positive years 1992, 2000 and 2004, and later blooms in NAO negative years 1995, 1998 and 2008. A negative trend between the NAO index and the initiation of the spring bloom (r=−0.32, $p < 0.2$), and a positive trend between SST and the initiation of the spring bloom (r=0.33, $p < 0.2$) were found for the study area (Table 1). Although the actual values of the initiation of the spring bloom revealed by the phytoplankton color index and satellite data are not strictly comparable, due to differences in temporal resolution within each dataset, they show generally similar trends from 1998 to 2003 and from 2006 to 2009 (Fig. 5). While the start date of the spring bloom estimated from two data sets differed by about 40 days from 2000 to 2003, the general direction in which the spring bloom timing changed from year to year was the same.

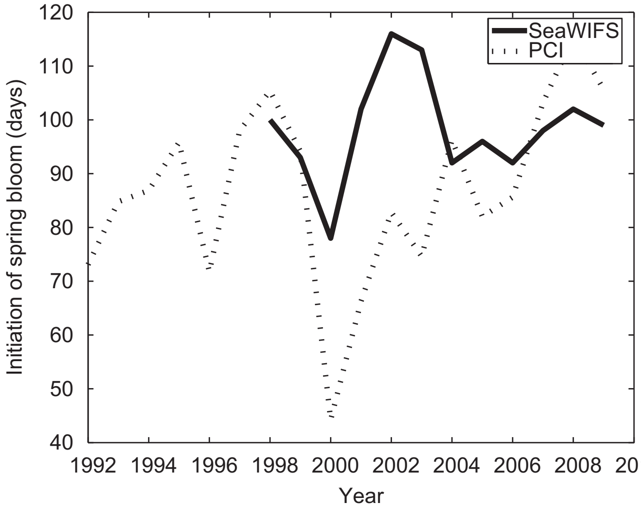

Fig. 5. The initiation of spring bloom derived from SeaWiFS chlorophyll-a (solid line) and phytoplankton color index (dashed line) data.

The phytoplankton community structure in the central North Atlantic was dominated by diatoms throughout much of the year with a shift in community composition favoring dinoflagellates in late summer, July to September. Seasonally the diatom ratio varied from 0.3 to 0.8, while the dinoflagellate ratio fluctuated between 0.2 and 0.4 (Fig. 6). The relative abundance of diatoms decreased during the period between 1991 and 2009, whereas the dinoflagellate ratio increased. Statistically significant correlations were found between the NAO, SST, diatom and dinoflagellate ratios (Fig. 7 and Table 1), with positive correlations observed between the NAO and the diatom ratio (r=0.70), SST and the dinoflagellate ratio ($r=0.63$), the diatom and dinoflagellate ratios ($r=0.9$) and negative correlations between the NAO and dinoflagellate ratio ($r=-0.63$), and SST and the diatom ratio ($r=-0.65$).

According to the AIC criterion (Table 2), the best model to explain variability in bloom timing includes the two explanatory variables SST and the NAO, but with a time lag of 1 year. The best model (Fig. 8) explains 34% of the observed variance, and the correlation between the estimated and observed bloom timing is 0.59 ($p<0.01$). Our analysis (Table 2) showed that adding the previous year's data improved the correlation between estimated and observed bloom

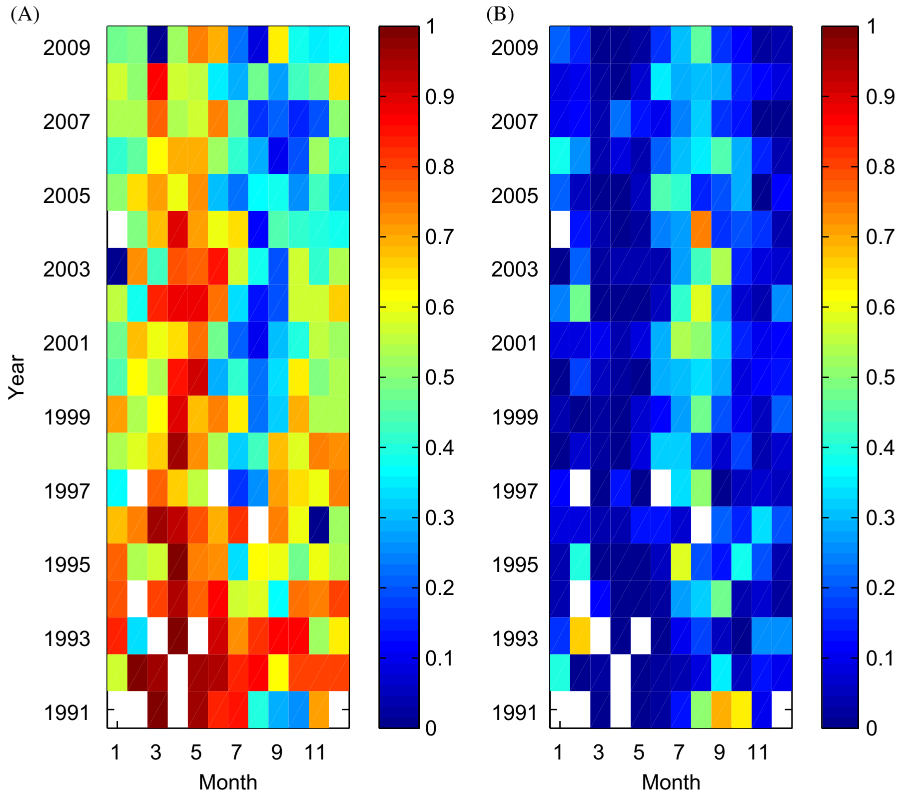

Fig. 6. (A) Mean monthly ratio of CPR diatom abundance to total phytoplankton abundance, and (B) Mean monthly ratio of CPR dinoflagellate abundance to total phytoplankton abundance from 1991–2009 for the central North Atlantic. White areas reflect the absence of CPR data available.

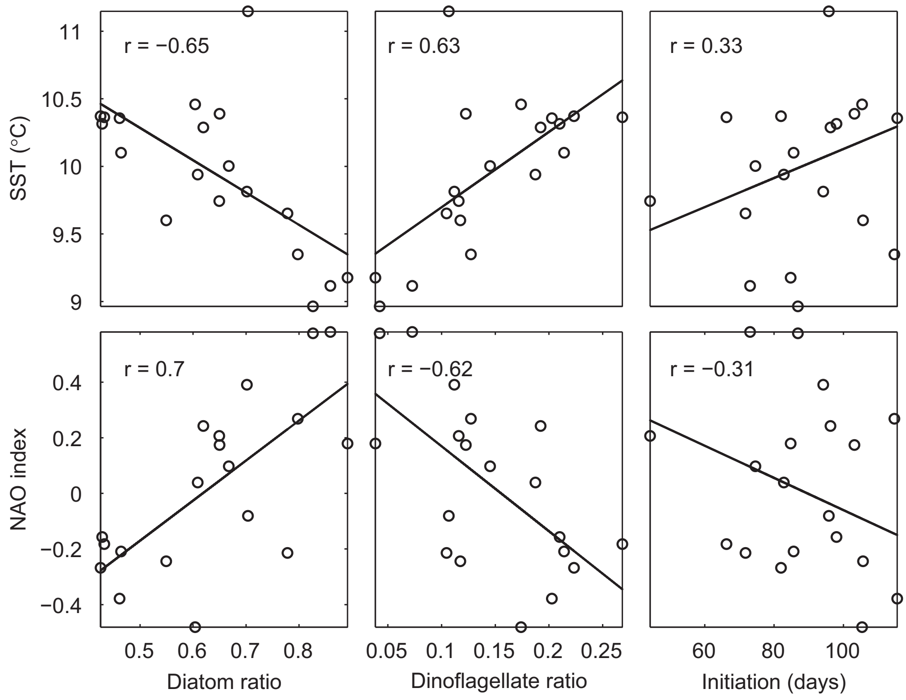

Fig. 7. Scatter plots of SST and CPR diatom ratio, SST and CPR dinoflagellate ratio, SST and initiation of the spring bloom derived from PCI, NAO and CPR diatom ratio, NAO and CPR dinoflagellate ratio, NAO and initiation of the spring bloom. The linear regression lines are shown in black.

timing. The best model for estimating diatom and dinoflagellate ratios included only the two explanatory variables SST and the NAO with no time lag (Fig. 8; Table 2). The model captured more than 50% of the observed variance, and the estimated ratios are significantly correlated with the observed ones ($r=0.7$, $p<0.001$). Lower SST and higher NAO index values resulted in a larger contribution of diatoms to total phytoplankton abundance. The diatom ratio was above 0.7 between 1992 and 1996, and fluctuated between 0.4 and 0.7 after 1997, whereas the dinoflagellate ratio was below 0.12 between 1992 and 1996, and above 0.11 after 1997. The retrospectively-estimated diatom ratio between 1985 and 1991 was higher than 0.6, however the dinoflagellate ratio was below 0.15. Phytoplankton community structure demonstrated a decadal decreasing trend in the diatom ratio and an increasing trend in the dinoflagellate ratio from 1985 to 2009, respectively. This reflects a real change in the relative abundance of diatoms and dinoflagellates, since the total phytoplankton taxa show no significant trend during this period (Head and Pepin, 2010b).

Table 2
Parameters and statistics for the regression models. The minimum AIC values are in bold.

c	a_0 (1/°C)	a_1 (1/°C)	b_0	b_1	κ^2	r	AIC
Diatom ratio							
0.63	0	0	0.34	0	0.49	0.70	−80.14
2.37	−0.17	0	0	0	0.42	0.65	−77.52
1.55	−0.09	0	0.24	0	0.56	0.75	**−80.22**
1.23	−0.09	0.03	0.23	0.15	0.60	0.78	−70.01
Dinoflagellate ratio							
0.15	0	0	−0.13	0	0.39	0.63	−109.60
−0.57	0.07	0	0	0	0.40	0.63	−109.90
−0.31	0.05	0	−0.08	0	0.49	0.70	**−110.13**
−0.53	0.05	0.01	−0.06	−0.02	0.54	0.73	−97.40
c (days)	a_0 (1/°C)	a_1 (1/°C)	b_0	b_1	κ^2	r	AIC
Initiation of spring bloom							
88.83	0	0	−12.96	0	0.05	0.22	113.21
22.78	6.60	0	0	0	0.04	0.20	113.37
53.96	3.49	0	−9.06	0	0.06	0.24	115.92
183.81	5.61	−15.14	−18.45	−35.79	0.35	0.59	**109.56**

4. Discussion

4.1. The NAO and sea surface temperature (SST)

The dominant mode of climate forcing in the North Atlantic is the North Atlantic Oscillation (NAO, Barnston and Livezey, 1987; Hurrell et al., 2003). The NAO is characterized by a north–south dipole pattern, being the only dipole structure found for every month of the year. The low pressure center is just west of Iceland near 70°N, and the center of opposite sign is found over the Atlantic near 35°N. A large positive NAO index is usually associated with strong westerly winds and a deepened Icelandic low. No preferred time scale of NAO variability is evident in time series of the NAO index (Hurrell et al., 2003). The NAO significantly affects sea surface temperature (SST), mixed-layer depth and mean circulation (Visbeck et al., 2003). The NAO index has been shown to influence the inter-annual variability of subpolar gyre (Deshayes and Frankignoul, 2008) and the transport in western Labrador Sea (Han and Tang, 2001).

The negative relationship between SST and the NAO in the north central Atlantic Ocean is similar to that presented in the early work of Visbeck et al. (2003), in which cooler temperatures were observed in the subpolar gyre region in winter seasons with a high NAO index. In a seminal paper, Bjerknes (1964) interpreted the changes in ocean temperatures as being partly due to the heat exchange at the air-sea interface, and partly due to advective heat transport by ocean currents. In a positive NAO index year, strong westerly winds increase the sensible heat loss from the ocean in the subpolar gyre through enhanced vertical mixing in the upper water column, thus lowering SST. In addition there is an enhanced equatorward Ekman transport of fresh water north of 40°N (Visbeck et al., 2003), and thus one could expect a decrease in SST and a southward movement of

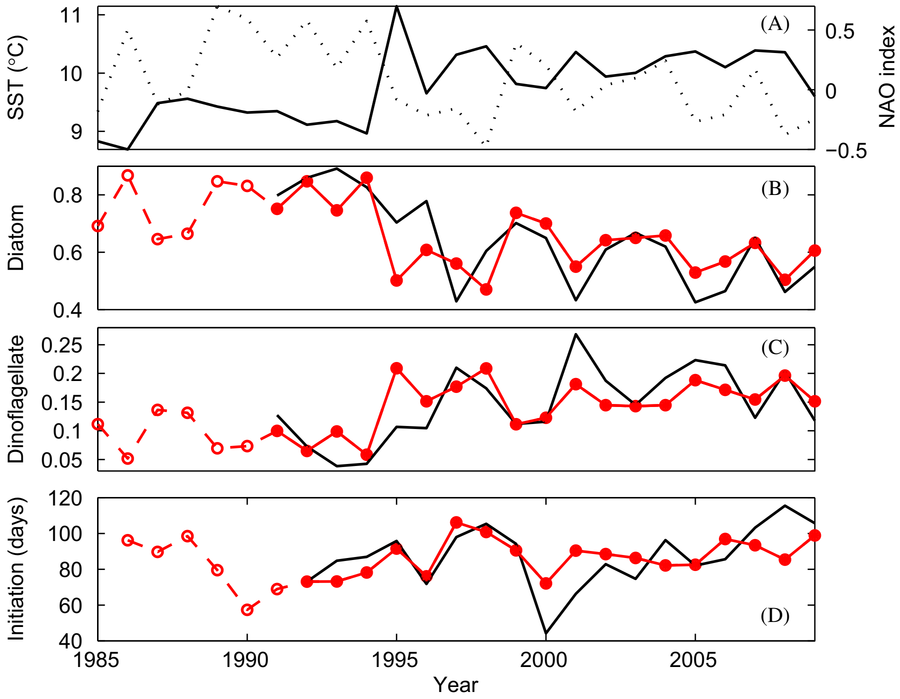

Fig. 8. Time series of (A) annual SST (solid line) and NAO index (dashed line) between 1985 and 2009, (B) ratio of CPR diatom abundance to total phytoplankton abundance (solid black line), estimated diatom ratio (solid dot line) and extrapolated diatom ratio (dashed dot line), (C) ratio of CPR dinoflagellate abundance to total phytoplankton abundance (solid black line), estimated dinoflagellate ratio (solid dot line) and extrapolated dinoflagellate ratio (dashed dot line), and (D) initiation of spring bloom computed by CPR PCI (solid black line), estimated initiation of the spring bloom (solid dot line) and extrapolated initiation of the spring bloom (dashed dot line).

the 9 °C isotherm, as seen in 1999. On the other hand, results of modeling studies suggest that SST anomalies have only a weak impact on the NAO on year-to-year time scales (Kushnir et al., 2002), but may have a strong impact on multidecadal variability of the winter NAO (Rodwell et al., 1999).

4.2. *Influence of the NAO on the initiation of the spring bloom*

Previous studies in this area (Platt et al., 2009; Zhai et al., 2011b, 2012) have shown that the spring bloom starts when the average light in the mixed-layer depth increases to a certain threshold in the Northwest Atlantic and around Iceland. Taylor and Ferrari (2011) have suggested that weaker turbulent mixing, resulting from a reduction in air-sea fluxes at the end of winter, triggered the onset of a spring bloom in the North Atlantic, although reduced mixing is functionally equivalent to increasing average light. Mahadevan et al. (2012) demonstrated that the initial stratification caused by eddy-driven slumping of the basin-scale north–south density gradient, resulted in an earlier spring bloom than would have occurred by seasonal warming in the subpolar North Atlantic. Collectively, these recent studies suggest that an underlying property controlling the initiation of spring blooms is vertical stratification. There are at least two possible scenarios affecting the stability of the upper water column in the central North Atlantic that can impact timing of spring bloom initiation (Taylor and Ferrari, 2011; Mahadevan et al., 2012). First is the reduction in vertical mixing dependent on wind stress, net heat flux, and the transport of different water masses in a horizontal direction. Second is, a “dilution-recoupling hypothesis” for phytoplankton blooms in the absence of spring mixed-layer shoaling (Behrenfeld 2010). The spring bloom in the study region occurs during a period of actively shallowing mixed-layer depth (Henson et al., 2006; Zhai et al., 2012; Mahadevan et al., 2012), and so Behrenfeld's hypothesis is unlikely to apply.

There are two competing mechanisms that affect the mixed-layer depth in the central North Atlantic. For a positive NAO index year, the vertical mixing induced by strong westerly winds deepens the mixed layer, whereas the enhanced southward transport of cold and fresh Arctic water promotes strong stratification and thus a shallow mixed-layer depth. Zhai et al. (2012) showed that Arctic water has a stable surface layer in comparison with the Atlantic water. A negative relationship between the NAO index and the onset of the spring bloom ($r= -0.32$, $p<0.2$), and a positive relationship between SST and the start date of the spring bloom ($r=0.33$, $p<0.2$) were found for the study area, indicating that horizontal transport may play a more important role than vertical mixing in affecting the onset of the spring bloom. The nominal relationship between the NAO, SST and the initiation of the spring bloom was found to be robust against the excessive influence of any particular data point. This was tested by removing single data points from the time series one at a time. The start date of the spring bloom is nominally correlated with the SST ($r=0.34$, $p<0.2$), and with the NAO ($r=-0.29$, $p<0.26$) when the earliest bloom point in 2000 was removed. However some previous studies (Henson et al., 2006, 2009) have shown that anomalous wind-driven mixing conditions can also influence the initiation of the spring bloom in the subpolar gyre.

4.3. *Effect of the NAO on phytoplankton community structure*

It has been shown that taxonomic composition varies with changes in physical forcing and nutrient availability (Platt et al., 2005). In general, diatoms dominate in nutrient-rich, turbulent waters, whereas dinoflagellates are characteristic of low-nutrient, highly-stratified waters (Margalef, 1978). Hence the transition from well-mixed winter water to stratified summer water is associated with a phytoplankton succession from diatoms to dinoflagellates, which was the case in the Northwest Atlantic Shelf (Head and Pepin, 2010a,b) and the Northeast Atlantic (Leterme et al., 2005; Henson et al., 2012). Head and Pepin (2010b) showed that in north central Atlantic Ocean, the annual means of absolute diatom abundance were consistently higher than those of dinoflagellate abundance, consistent with the findings of this study (Fig. 6). These elevated diatom abundances may be influenced by a persistent Sub-Polar Front. Tilstone et al. (in preparation) found that the primary production at the Sub-Polar Front is much higher than in other regions.

Phytoplankton taxonomic structure is correlated with the physical forcing of the NAO, with a positive correlation between the NAO and diatom ratio ($r=0.70$), and a negative correlation between the NAO and dinoflagellate ratio ($r=-0.63$, Fig. 7, Table 1). The link between phytoplankton community structure and SST has been shown repeatedly in the literature (Bouman et al., 2003; Platt et al., 2005), but fewer studies have demonstrated the quantitative relationship between the NAO index and CPR phytoplankton taxonomic groups. A possible explanation for this relationship lies in the link between nutrient supply to the surface layer associated with NAO forcing and temperature. SST provides a quantitative index of physio-chemical state of the marine environment. The strong westerly wind-induced mixing during the high NAO index years causes an increase in the vertical flux of nutrients from below the mixed layer in the NADR province, and an increase in the horizontal transport of nutrients in the ARCT province (Oschlies, 2001); conditions that would favor increased relative abundance of diatoms. Low SST is associated with a weakening in the density gradient (stratification) and a corresponding increase in the diffusion of nutrients across the pycnocline, creating a favorable environment for diatoms.

4.4. *Retrospective estimation of phytoplankton inter-annual variability*

The importance of the statistical relationship between phytoplankton and physical forcing is that the inter-annual variability in phytoplankton could be estimated retrospectively using readily-available physical variables. Yamada and Ishizaka (2006) used the wind speed to extrapolate the timing of the spring bloom back to the mid-1980s in Japan Sea. Raitsos et al. (2005) extended the SeaWiFS chlorophyll record back 50 years in the northeast Atlantic. In their studies, only one variable was used as a predictor in the linear regression model. In our study, we compared four models containing from 1 to 4 explanatory variables, with better results than Sameoto (2001) in estimating phytoplankton community structure. Our analysis shows that adding previous year's data improves the correlation between estimated and observed bloom initiation ($r=0.59$, $p<0.01$). A possible explanation is that the initiation of the spring bloom depends on the fresh water transport in the previous year. The positive NAO phase is associated with significant freshening along the North Atlantic Current as well as the East and West Greenland currents (Visbeck et al., 2003). The positive NAO-induced surface Ekman transport enhances the fresh water fluxes in the region, resulting in stronger stratification and a shallower mixed layer depth in the following spring. Therefore the initiation of the spring bloom can be estimated from the proceeding year's NAO index. This suggests the regression model could be used as a tool to fill the gaps in CPR data for the 1980s, during which the CPR sampling was temporarily terminated.

The extrapolated initiation of the spring bloom (Fig. 8D) showed late spring blooms in mid-1980s, which were captured by a biogeochemical and ocean ecosystem model (Henson et al., 2009). Henson et al. (2009) observed a gradual delay of 30 days from an earlier to a later spring bloom during the period between 1985 and 1989 in the transition zone between subpolar and subtropical waters. During this period, the general increasing trend in the NAO index results in significant freshening in the study region, which is expected to enhance stratification and promote earlier spring blooms.

The two-variable regression model forced by the NAO and SST explained 50% of the inter-annual variance of the diatom ratio and dinoflagellate ratios, and revealed a decadal decreasing trend in the diatom ratio, and an increasing trend in the dinoflagellate ratio between 1985 and 2009 in the north central Atlantic (Fig. 8B and C). The possible reasons for these trends relate to the downward trend in the annual NAO indices and upward trend in the annual SST (Fig. 8A), which indicate stronger stratification. This decrease in the NAO index is associated with the weakening of the westerly wind, which reduces vertical mixing leading to decreased turbulence. As turbulent environments are generally associated with diatoms and calm conditions with dinoflagellates, it is perhaps not unexpected that the relative abundance of diatoms versus dinoflagellates decreased between 1985 and 2009 in the north central Atlantic Ocean. Head and Pepin (2010a), their Fig. 3, also indicated a similar decreasing trend in the region, though the inter-decadal changes in the abundance of diatoms and dinoflagellates are generally insignificant. This is in contrast to a marked increase in the relative abundance of diatoms versus dinoflagellates since 1995 observed in the northeast Atlantic using CPR samples (Fig. 1C in Hinder et al., 2012), which is driven by the interaction of increasing SSTs combined with increasing summer winds favoring turbulent environments.

This study demonstrated that variations in the phytoplankton community structure and the initiation of the spring bloom can be inferred from changes in the climatic forcing of the NAO over the North Central Atlantic. Because the NAO can simultaneously increase ocean temperatures in one part of the Atlantic basin and reduce them in another, the effect of modulations on the time of onset of phytoplankton blooms and community structures can vary geographically and requires detailed examinations in different regions. The complex and differential responses of the surface layers of the North Atlantic Ocean to NAO forcing have been elucidated (Visbeck et al., 2003): our study implies that the linkages between the NAO, and changes in stratification and phytoplankton processes are expressed at the entire basin scale of the North Atlantic.

Acknowledgments

This work has been supported by the Canadian Space Agency. This paper was first presented in the Plankton 2011 symposium to celebrate 80 years of the Continuous Plankton Recorder Survey held in Plymouth, UK. Discussions with Venetia Stuart and Eric Head have helped improve the paper. The constructive comments by two anonymous reviewers are greatly appreciated.

References

Akaike, H., 1974. A new look at the statistical model identification. IEEE Trans. Autom. Control 19 (6), 716–723.

Barnston, A.G., Livezey, R.E., 1987. Classification, seasonality and persistence of low-frequency atmospheric circulation patterns. Mon. Wea. Rev. 115, 1083–1126.

Barton, A.D., Greene, C.H., Monger, B.C., et al., 2003. The Continuous Plankton Recorder survey and the North Atlantic Oscillation: interannual to multidecadal-scale patterns of phytoplankton variability in the North Atlantic Ocean. Prog. Oceanogr. 58, 337–358.

Batten, S.D., Walne, A.W., Edwards, M., et al., 2003a. Phytoplankton biomass from continuous plankton recorder data: an assessment of the phytoplankton colour index. J. Plankton Res. 7, 697–702.

Batten, S.D., Clarke, R., Flinkman, J., Hays, G., John, E., John, A.W.G., Jonas, T.D., Lindley, J.A., Stevens, D., Walne, A., 2003b. CPR sampling: the technical background, materials and methods, and issues of consistency and comparability. Prog. Oceanogr.0079-661158, 193–215.

Behrenfeld, M.J., 2010. Abandoning Sverdrup's Critical Depth Hypothesis on phytoplankton blooms. Ecology 91 (4), 977–989.

Bjerknes, J., 1964. Atlantic air–sea interactions. Adv. Geophys. 10, 1–82.

Bouman, H.A., Platt, T., Sathyendranath, S., Li, W.K.W., Stuart, V., Fuentes-Yaco, C., Maass, H., Horne, E.P.W., Ulloa, O., Lutz, V., Kyewalyanga, M., 2003. Temperature as indicator of optical properties and community structure of marine phytoplankton: implications for remote sensing. Mar. Ecol. Prog. Ser. 258, 19–30.

Burnham, K.P., Anderson, D.R., 2004. Multimodel inference: understanding AIC and BIC in Model Selection. Sociol. Methods Res. 33, 261–304.

Colebrook, J.M., Robinson, G.A., 1961. The seasonal cycle of the plankton in the North Sea and the North-East Atlantic. J. Cons. Int. Explor. Mer. 26, 156–165.

Colebrook, J.M., Robinson, G.A., 1965. Continuous plankton records: seasonal cycles of phytoplankton and copepods in the northeastern Atlantic and North Sea. Bull. Mar. Ecol. 6, 123–139.

Deshayes, J., Frankignoul, C., 2008. Simulated variability of the circulation in the North Atlantic from 1953 to 2003. J. Clim. 21, 4919–4933.

Devred, E., Sathyendranath, S., Platt, T., 2007. Delineation of ecological provinces in the North West Atlantic using visible spectral radiometry (ocean colour). Mar. Ecol. Prog. Ser. 346, 1–13.

Edwards, M., Richardson, A.J., 2004. Impact of climate change on marine pelagic phenology and trophic mismatch. Nature, 881–884.

Fox, J., 2008. Applied Regression Analysis and Generalized Linear Models, 2nd ed. SAGE Publications, Inc.688.

Han, G., Tang, C.L., 2001. Interannual variation of volume transport in the western Labrador Sea based on TOPEX/Poseidon and WOCE data. J. Phys. Oceanogr. 31, 199–211.

Head, E.J.H., Sameoto, D.D., 2007. Inter-decadal variability in zooplankton and phytoplankton abundance on the Newfoundland and Scotian shelves. Deep-Sea Res. II 54, 2686–2701.

Head, E., Pepin, P., 2010a. Spatial and inter-decadal variability in plankton abundance and composition in the Northwest Atlantic (1958–2006). J. Plankton Res. 32, 1633–1648.

Head, E., Pepin, P., 2010b. Monitoring changes in phytoplankton abundance and composition in the Northwest Atlantic: a comparison of results obtained by continuous plankton recorder sampling and colour satellite imagery. J. Plankton Res. 32, 1649–1660.

Henson, S., Robinson, I.S., Allen, J.T., Waniek, J.J., 2006. Effect of meteorological conditions on interannual variability in timing and magnitude of the spring bloom in the Irminger Basin, North Atlantic. Deep-Sea Res. I 53, 1601–1615 http://dx.doi.org/10.1016/j.dsr.2006.07.009.

Henson, S.A., Dunne, J.P., Waniek, J.J., 2009. Decadal variability in North Atlantic phytoplankton blooms. J. Geophys. Res., 114, http://dx.doi.org/10.1029/2008JC005139.

Henson, S., Lampitt, R., Johns, D., 2012. Variability in phytoplankton community structure in response to the North Atlantic Oscillation and implications for organic carbon flux. Limnol. Oceanogr. 57 (6), 1591–1601, http://dx.doi.org/10.4319/lo.2012.57.6.1591.

Hinder, S.L., Hays, G.C., Edwards, M., Roberts, E.C., Walne, A.W., Gravenor, M.B., 2012. Changes in marine dinoflagellate and diatom abundance under climate change. Nat. Clim. Change 2, 271–275, http://dx.doi.org/10.1038/nclimate1388.

Hurrell, J.W., Kushnir, Y., Ottersen, G., Visbeck, M., 2003. The North Atlantic oscillation climatic significance and environmental impact, Geophysical Monograph. American Geophysical Union, Washington, DC, USA279.

Koeller, P., Fuentes-Yaco, C., Platt, T., Sathyendranath, S., Richards, A., Ouellet, P., Orr, D., Skúladóttir, U., Wieland, K., Savard, L., Aschan, M., 2009. Basin-Scale coherence in phenology of shrimps and phytoplankton in the North Atlantic Ocean. Science, 324, http://dx.doi.org/10.1126/science.1170987.

Kushnir, Y., Robinson, W.A., Bladé, I., Hall, N.M.J., Peng, S., Sutton, R., 2002. Atmospheric GCM response to extratropical SST anomalies: synthesis and evaluation. J. Clim. 15, 2233–2256.

Leterme, S.C., Edwards, M., Seuront, L., Attrill, M.J., Reid, P.C., John, A.W.G., 2005. Decadal basin-scale changes in diatoms, dinoflagellates, and phytoplankton color across the North Atlantic. Limnol. Oceanogr. 50, 1244–1253.

Longhurst, A., 2007. Ecological Geography of the Sea, 2nd ed. Elsevier, San Diego, CA 542 pp.

Mahadevan, A., D'Asaro, E., Lee, C., Perry, M.J., 2012. Eddy-driven stratification initiates North Atlantic Spring phytoplankton blooms. Science 337, 54, http://dx.doi.org/10.1126/science.1218740.

Margalef, R., 1978. Life-forms of phytoplankton as survival alternatives in an unstable environment. Oceanol. Acta 1, 493–509.

O'Reilly, J.E., Maritorena, S., Mitchell, B.G., et al., 1998. Ocean colour algorithms for SeaWiFS. J. Geophys. Res. 103, 13279–13294.

Oschlies, A., 2001. NAO-induced long-term changes in nutrient supply to the surface waters of the North Atlantic. Geophys. Res. Lett. 28, 1751–1754.

Platt, T., Sathyendranath, S., 1999. Spatial structure of pelagic ecosystem processes in the global ocean. Ecosystem 2, 384–394.

Platt, T., Fuentes-Yaco, C., Frank, K.T., 2003. Spring algal bloom and larval fish survival. Nature 423, 398–399.

Platt, T., Bouman, H., Devred, E., Fuentes-Yaco, C., Sathyendranath, S., 2005. Physical forcing and phytoplankton distributions. Sci. Mar. 69, 55–73.

Platt, T., Sathyendranath, S., 2008. Ecological indicators for the pelagic zone of the ocean from remote sensing. Remote Sens. Environ. 112, 3426–3436.

Platt, T., Sathyendranath, S., White, G., Fuentes-Yaco, C., Zhai, L., Devred, E., Tang, C., 2009. Diagnostic properties of phytoplankton time series from remote sensing. Estuar. Coasts, http://dx.doi.org/10.1007/s12237-009-9161-0.

Racault, Marie-Fanny, Le Quéré, Corinne, Buitenhuis, Erik, Sathyendranath, Shubha, Platt, Trevor, 2012. Phytoplankton phenology in the global ocean. Ecol. Indicators 14 (1), 152–163 10.1016/j.ecolind.2011.07.010.

Raitsos, D.E., Reid, P.C., Lavender, S.J., Edwards, M., Richardson, A.J. Extending, 2005. The SeaWiFS chlorophyll data set back 50 years in the northeast Atlantic. Geophys. Res. Lett. 32, L06603.

Raitsos, D.E., Lavender, S.J., Pradhan, Y., Tyrell, T., REID, P.C., Edwards, M., 2006. Coccolithophore bloom size variation in response to the regional environment of the subarctic North Atlantic. Limnol. Oceanogr. 51, 2122–2130.

Reid, P.C., Edwards, M., Hunt, H.G., Warner, A.J., 1998. Phytoplankton change in the North Atlantic. Nature 391, 546.

Richardson, A.J., Walne, A.W., John, A.W.G., Jonas, T.D., Lindley, J.A., Sims, D.W., Stevens, D., Witt, M., 2006. Using continuous plankton recorder data. Prog. Oceanogr. 0079-661168 (1), 27–74.

Rodwell, M.J., Rowell, D.P., Folland, C.K., 1999. Oceanic forcing of the winter time North Atlantic Oscillation and European climate. Nature 398, 320–323.

Sameoto, D., 2001. Decadal changes in phytoplankton color index and selected calanoid copepods in continuous plankton recorder data from the Scotian Shelf. Can. J. Fish. Aquat. Sci. 58, 749–761.

Sverdrup, H.U., 1953. On conditions for the vernal blooming of phytoplankton. J. Cons. Permanent Int. pourl'Explor. de la Mer 18, 287–295.

Taylor, J., Ferrari, R., 2011. A shutdown of turbulent convection can trigger the spring phytoplankton bloom. L & O 56, 2293–2307.

Tilstone G.H., Miller P.I., Brewin R., and Priede I.G., 2013. Enhancement of primary production in the North Atlantic outside of the spring bloom. Remote Sensing Environ., in preparation.

Visbeck, M., Chassignet, E.P., Curry, R.G., Delworth, T.L., Dickson, R.R., and Krahmann, G., 2003. The Ocean's response to North Atlantic Oscillation Variability *in* The North Atlantic Oscillation: climatic significance and environmental impact. Geophysical Monograph 134, AGU, pp. 113–145.

Yamada, K., Ishizaka, J., 2006. Estimation of interdecadal change of spring bloom timing; in the case of the Japan Sea. Geophys. Res. Let. 33, L02608, http://dx.doi.org/10.1029/2005GL024792.

Zhai, L., Platt, T., Tang, C., Sathyendranath, S., Fuentes-Yaco, C., Devred, E., Wu, Y.S., 2010. The seasonal and geographic variations of phytoplankton losses from the mixed layer on the Northwest Atlantic Shelf. J. Mar. Syst. http://dx.doi.org/10.1016/j.jmarsys.2009.09.005.

Zhai, L., Tang, C., Platt, T., Sathyendranath., S., 2011a. Ocean response to attenuation of visible light by phytoplankton in the Gulf of St. Lawrence. J. Mar. Syst. 88, 285–297.

Zhai, L., Platt, T., Tang, C., Sathyendranath, S., Hernández Walls, R., 2011b. Phytoplankton phenology on the Scotian Shelf. ICES J. Mar. Sci. 68, 781–791.

Zhai, L., Gudmundsson, K., Miller, P., Peng, W.J., Gudfinnsson, H., Debes, H., Hatun, H., White III, G.N., Hernandez Walls, R., Sathyendranath, S., Platt, T., 2012. Phytoplankton phenology and production around Iceland and Faroes. Cont. Shelf. Res. 37 (1), 15–25.